A Method of Feature Extraction from Time-Frequency Images of Vibration Signals in Faulty Bearings for Classification Purposes

Dorel Aiordachioaie
”Dunarea de Jos” University of Galati
Electronics and Telecom. Department
Galati, Romania
e-mail: Dorel.Aiordachioaie@ugal.ro

Theodor D. Popescu
National Institute for Research
and Development in Informatics
Bucharest, Romania
e-mail: Theodor.Popescu@ici.ro

Bogdan Dumitrascu
”Dunarea de Jos” University of Galati
Electronics and Telecom. Department
Galati, Romania
e-mail: Bogdan.Dumitrascu@ugal.ro

***Abstract*—Time-frequency image processing is considered in the context of change detection and diagnosis purposes of bearings with faults and vibration signal processing. The analysis of these images reveals some difficulties in obtaining accurate results in classification. Some images are different compared to other images from the same set. New images are obtained by applying a criterion based on the contours generated by the main components of the analyzed time-frequency image. The transformed images are less complex, and could be with white and black only. Features based on statistical moments are considered, selected and used to define discriminant functions, which could improve the results of the classification. The features include the number of the contours, the average area defined by the contours, the variance of the areas and the Renyi entropies.**

Keywords-signal; vibration; image; time-frequency transform; signal processing; feature selection; classification.

I. INTRODUCTION

An important activity in industry, for safe work and quality of the products, is the Change Detection and Diagnosis (CDD) of various processes. These two activities are parts of wider domain, called condition-based and predictive maintenance, as described in some excellent books with theory and applications [1] [2] [3]. In the field of vibrational processes, i.e., processes which generates mechanical vibrations, with or without faults or damages, advanced signal processing algorithms are intensively used to elaborate accurate and robust algorithms for process diagnosis [4] [5] [6].

One of the more complex signal processing method is based on time-frequency transform, and next on time-frequency images, as described in [7] [8] [9]. The structure of such processing chain is presented in Figure 1. Signals from the process under study are pre-processed both on continuous and discrete time, mainly by filtering and scaling. Next, a time sliding window is considered for the computation of the time-frequency transform. The parameters of the sliding window depend on the statistical properties of the analyzed signals, to meet the condition of the statistical stationarity. The coefficients of the time-frequency transform are considered as elements of an image. From this point all processing steps are based on image processing, for various tasks, as fault detection and diagnosis.

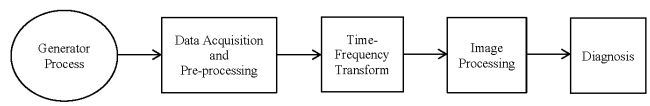

Figure 1. The block structure of signal processing for CDD

This work considers the last block before diagnosis, i.e., image processing for classification purposes. The previous processing blocks, mainly for signal processing, i.e., data acquisition and pre-processing, time-frequency transforms, are described in the Sections of the paper. Direct classification of time-frequency images do not offer always the best results in CDD activities, as described in [10] [11]. It is the main objective of this paper to define algorithms for feature selection and extraction, in order to expect better results of the classification and diagnosis purposes.

The rest of this paper is organized as follows. Section II describes the basic transforms applied to the vibrating signals, i.e., time-frequency and Renyi entropy. Section III describes the data which was used for experiments, including time-frequency images. Section IV addresses the proposed method for feature selection. Section V goes into the results of the experiments. The conclusion and acknowledgement close the article.

II. SIGNAL TRANSFORMS

Signal transforms are used to compute specific features of the analyzed signal or to change the analysis system, e.g., time-frequency transforms, or to compute and extract other relevant features, e.g., the Renyi entropy.

A. Time-Frequency Transform

Time-frequency transforms are advanced processing techniques for data processing, and especially for data coming from non-stationary signals. A general theoretical framework is presented in [12] [13]. Examples of signals and applications are audio signals [14], mechanical vibrations [15] or biomedical signals [16].

If $x(t)$ is a continuous (possible complex) signal, the time-frequency transforms can be obtained from the general formula [20]

$$C_x(t,\omega) = \frac{1}{4\pi^2}\iiint x\left(t+\frac{\tau}{2}\right)x^*\left(t-\frac{\tau}{2}\right)\phi(\theta,\tau) \cdot e^{-j\theta t - j\omega\tau + j\theta u}\, du\, d\tau\, d\theta \quad (1)$$

where $\phi(\theta,\tau)$ is the kernel function, which imposes the properties of the distribution, and "*" denotes complex conjugation. If the kernel function is 1, then the Wigner distribution is obtained.

For the case where *x(t)* is an analytical signal, the Wigner distribution is called the Wigner-Ville distribution (WVD) [17]. This distribution satisfies a large number of desirable mathematical properties, as described in the specialized literature [18] [19]. In particular, the WVD is always real-valued; it preserves time and frequency shifts and satisfies the marginal properties. It has also some drawbacks, as the apparition of the cross-terms. This is the reason for using the Choi-Williams Distribution (CWD) where the kernel function is [12]

$$\phi(\theta,\tau) = \exp\left[-(\theta\tau)^2/\sigma^2\right] \quad (2)$$

This distribution function adopts exponential kernel to suppress the cross-term that results from the components that differ in both time and frequency centers.

The discrete WVD is defined by [13]

$$W(n,m) = \frac{1}{2N}\sum_{k=0}^{N-1} x(kT) \cdot x^*((n-k)T)\cdot \exp\left(-\frac{j\pi\cdot m\cdot(2k-n)}{N}\right) \quad (3)$$

It is informal to verify that *W(n,m)* is a periodic function of period $2N$ in both time and frequency. The last relationship shows that in the range $0 \le n < 2N-1,\ 0 \le m < 2N-1$, representing one period, the WVD needs only be calculated over the range $0 \le n < N-1,\ 0 \le m < N-1$, having an area of one quarter that of the complete period.

The coefficients of the time-frequency transform define an image, which will be called a Time-Frequency Image (TFI).

B. Entropy Transform

The objective of the section is to introduce a criterion to describe the time-frequency images, from content point of view, before measuring the similarities for classification purposes. The start point is the registration process of the image, as pre-processing step before classification of these images.

Common algorithms for image registration could use: translation, on *x* and *y* directions; rigid processing, which means translation plus rotation; similarity, which means translation, rotation and scaling; affine transformation, which considers translation, rotation, scaling, and shearing. The choice of one of them is based mainly on the content of the image, the sources and the number of the images which are considered for registration. Simple registration methods of the images, from the content point of view, use intensity-based registration algorithms. As complexity rises, feature-based is more indicated. Details and examples are available in many references [20] [21].

The registration time is rapidly growing from translation to affine transformation. Sometimes, for complex transforms - like affine, the registration process could diverge. This is the reason to consider new methods valid for time-frequency images – in general – and in the case of bearings, in particular. The proposed procedure considers a number of maxima which will be considered as reference, i.e., their positions remain unchanged during and after registration.

Based on the above remarks, a criterion based on the image similarity is promoted, in order to select/decide if an image of the set could be registered or not. In principle, if the similarity with the reference image is low, then the registration of that image is skipped. The similarity is evaluated based on information content with the help of Renyi entropy. Definition of the alpha order Renyi entropy from [22] is considered as

$$HR_\alpha(\mathbf{I}) = -\frac{1}{1-\alpha}\log_2 \iint\left(\frac{I(t,f)}{\iint I(u,v)\,du\,dv}\right)^\alpha dt\,df \quad (4)$$

By discretization of this measure by setting $t = n\cdot\Delta t$ and $f = k\cdot\Delta f,\ n,k \in Z$ yields

$$HR_\alpha(\mathbf{I}) = -\frac{1}{1-\alpha}\log_2 \sum\sum\left(\frac{I[n,k]}{\sum\sum I[n',k']}\right)^\alpha + \log_2(\Delta t\cdot\Delta f) \quad (5)$$

Depending on the processed data, a number of images from the data set will be discarded, i.e., not considered for the registration step, as in [24]. The rejected images have very low similarity comparing with the prototype of the considered set and could come from some transient processes during the raw signal acquisition stage.

III. Data Description and Image Analysis

Data were considered for the case of faults in bearings, available from [23], and briefly described in Table I. Three types of faults are available, like F1 (Inner race), F2 (Ball) and F3 (Outer race). The case F0 means no faults. Vibration data from four sizes of the faults are available. The data set has the advantage of consistency, by considering faults from incipient/small size (0.007") to a larger one (0.028").

The sampling rate is 12,000 Hz, the motor load is 0 hp, and all data are from drive end bearing (DE). A set of four classes of patterns are considered as: C#0 – no faults, defined by d0; C#1 –inner race, defined by {**d1, d6, d9, d14**}; C#2 – ball, defined by {**d2, d7, d10, d15**}; C#3-outer race defined by {**d3, d8, d11**}. The vectors **d4, d5, d12**, and **d13** correspond to other sites of the transducers.

TABLE I. DATA TEST SET

Fault size	Faults			
	F0	**F1**	**F2**	**F3**
	Free	**Inner Race**	**Ball**	**Outer Race**
0.000“	**d0**	-	-	-
0.007"	-	**d1**	**d2**	**d3, d4, d5**
0.014"	-	**d6**	**d7**	**d8**
0.021"	-	**d9**	**d10**	**d11, d12, d13**
0.028"	-	**d14**	**d15**	-

IV. THE PROPOSED METHOD

Taking into account the results obtained by other methods, e.g., [10] [11], a method to select the important features of the time-frequency image and to define a new set of features, is developed. The method considers the content of the image by taking images with a pre-defined number of peaks, e.g., 1 to 3, depending on the complexity of the image. Thus, a new image is considered and defined in terms of contours, defined by the above peaks, which will be called transformed images or contour-based images (CBI).

In the set of the four next figures, i.e., Figure 2 to Figure 5, the raw/original images and the transformed images are presented, for all four classes, i.e., *C*#1 to *C*#4. On blue background, the set of the registered images are presented. Registration is made on the set of the images obtained from the frames of each record/file, as described in [24]. These images are considered as the prototypes of the classes.

The transformed images are presented on white background. A primary analysis of these images reveals some interesting properties:

a) the common content of the images is of vertical lines, as C#1(1,6,9), C#3(3,11,12);
b) the class C#2 has a very complex patterns, for all cases (2,7,10, and 15);
c) The classes C#1 and C#3 have some strange patterns, C#1(14) and C#3(8). Keeping all these images will damage the final classification, so images with high dissimilarity are removed from processing.

In order to extract the right information/features from the transformed images, the following elements are considered in defining the necessary features for classifications:

i) the number of contours, *Nc*, as a measure of the complexity;
ii) the area of the polygons, *Ac*, as a measure of the spreading on horizontal plane;
iii) the variance of the above areas, *var(Ac)*, as a measure of the complexity;
iv) the average of the area of the polygons, $E\{A_c\}$;
v) the mean of the squared values of areas, $E\{A^2_c\}$;
vi) the Renyi entropy of transformed images, *RH*.

A vector of features could be defined by using the above variables, as

$$\mathbf{f}_i = \left[N_c \quad \sum A_c \quad \mathrm{var}(Ac) \quad \overline{A_c} \quad \overline{A_c^2} \quad RH \right], \quad i = 1,2,3,4 \tag{6}$$

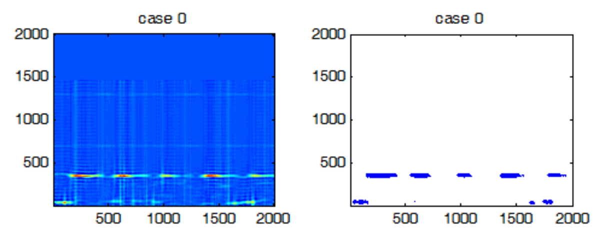

Figure 2. Class #0. Original and transformed image.

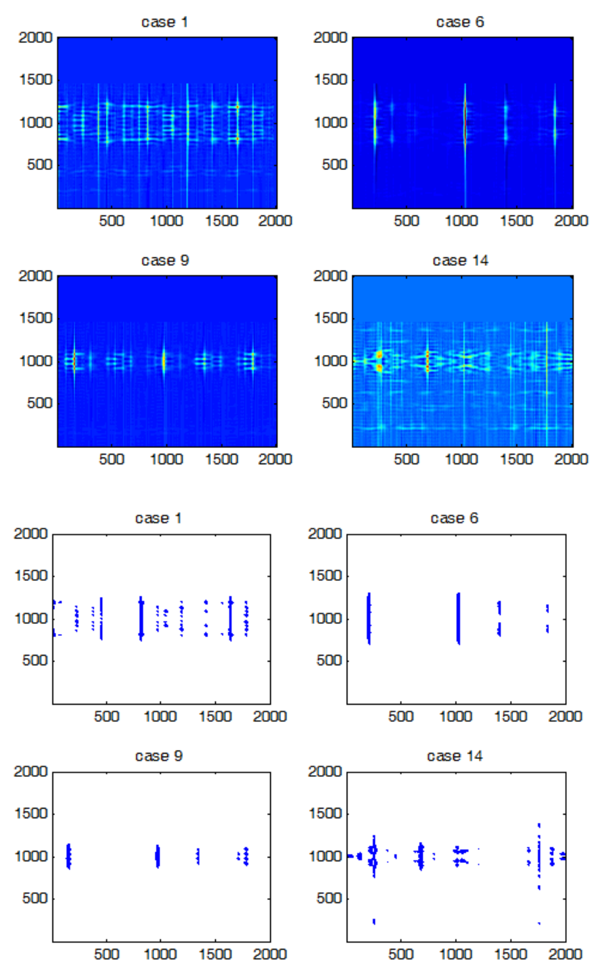

Figure 3. Class #1. Original and transformed images.

For each data vector **d** from a class, the vector $\mathbf{f}_i$ is evaluated, and matrix of features is obtained for each class, as

$$\mathbf{F}_j = [\mathbf{f}_1 \quad \mathbf{f}_2 \quad \ldots \quad \mathbf{f}_4],\ j = \overline{1,4} \tag{7}$$

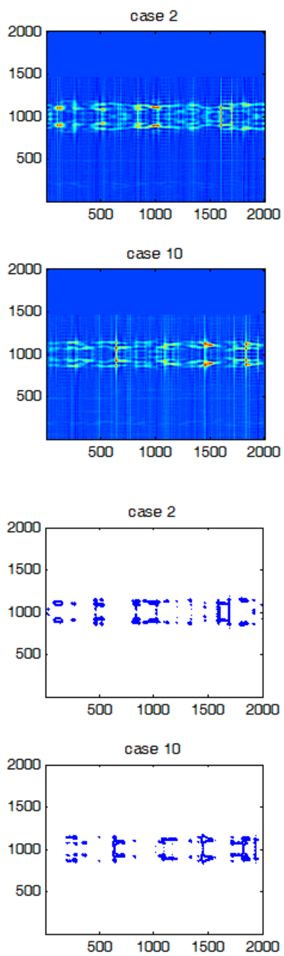

Figure 4. Class #2. Original and transformed images

The effect of the features is estimated by a general discriminant matrix

$$D(k,j) = \sum_{k=0}^{3}\sum_{j=0}^{3}(\mathbf{F}_k - \mathbf{F}_j)^2, k, j = \overline{1,4} \tag{8}$$

or, by considering only the distinct classes, by the discriminant functions

$$D_m = E\{D(k,j) \mid k \neq j, k > j, k, j = \overline{1,4}\} \tag{9}$$

or

$$D_v = \mathrm{var}\{D(k,j) \mid k \neq j, k > j, k, j = \overline{1,4}\} \tag{10}$$

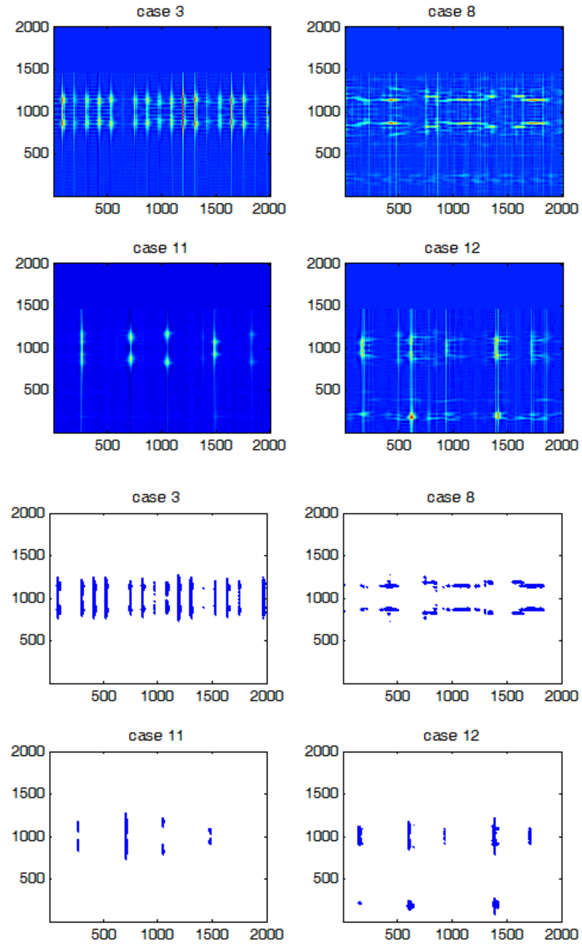

Figure 5. Class #3. Original and transformed images.

V. RESULTS OF THE EXPERIMENTS

From various experiments, the best results are presented in Table II. Figure 6 presents the features space, composed from the first three normalized features, and the values of the discriminant functions. The best structure of the feature vector, as result of the maximum variance, ***Dv***, is offered on the first line with a value of 6.23.

TABLE II. DISCRIMINANT VALUES

No	*Feature vector*	*Dm*	*Dv*
1	$[\mathbf{N_c} \quad \overline{\mathbf{A_c}} \quad \overline{\mathbf{A_c^2}} \quad \mathbf{RH}]$	3.88	6.23
2	$[\mathbf{N_c} \quad \overline{\mathbf{A_c}} \quad \mathrm{var}(Ac) \quad \mathbf{RH}]$	3.79	5.64
3	$[\mathbf{N_c} \quad \overline{\mathbf{A_c}} \quad \mathrm{var}(Ac) \quad \sum Ac]$	4.34	4.33

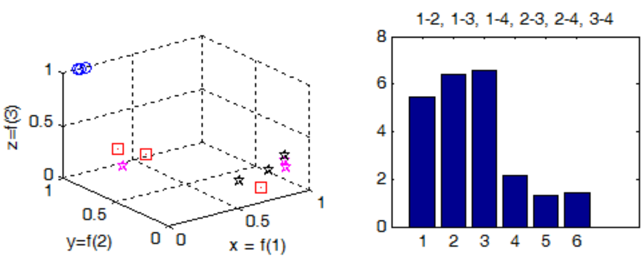

Figure 6. Feature space and the discriminant values

The unnormalized values are presented in the following. A column is used for a class. The first column is for class #0, i.e., free of faults. The next column are for classes 1, 2 and 3. For class C#0, because only one vector is available, the next three vectors are considered identically with the first one.

J1m =

23	150	179	204
23	25	86	138
23	16	173	12
23	143	48	69

J2m =

896.10	94.20	184.68	200.69
896.10	405.73	143.06	181.46
896.10	539.86	191.68	465.38
896.10	128.87	457.87	180.73

J3m = 1.0e+06 *

3.1544	0.2217	0.4132	0.5623
3.1544	1.3166	0.4640	0.3623
3.1544	1.3451	0.7012	0.9783
3.1544	0.5633	1.3616	0.4031

J4m =

4.4006	6.0824	5.9316	5.6459
4.4006	4.2532	5.8992	6.1837
4.4006	4.6008	5.7734	4.0958
4.4006	6.2462	5.3046	5.4525

Next, the features are organized in classes, one column for a parameter, and one line for a data vector of the same class. In this way, the parametric matrices from PC1 to PC4 are obtained and used in the computation of the discriminant functions.

PC1 =

0.1127	1.0000	1.0000	0.7235
0.1667	1.0000	1.0000	0.7116
0.1329	1.0000	1.0000	0.7622
0.1608	1.0000	1.0000	0.7045

PC2 =

0.7353	0.1051	0.0703	1.0000
0.1812	0.4528	0.4174	0.6878
0.0925	0.6025	0.4264	0.7969
1.0000	0.1438	0.1786	1.0000

PC3 =

0.8775	0.2061	0.1310	0.9752
0.6232	0.1596	0.1471	0.9540
1.0000	0.2139	0.2223	1.0000
0.3357	0.5110	0.4317	0.8492

PC4 =

1.0000	0.2240	0.1783	0.9282
1.0000	0.2025	0.1148	1.0000
0.0694	0.5193	0.3101	0.7094
0.4825	0.2017	0.1278	0.8729

VI. CONCLUSION

The objective of the paper was to find a solution to the classification problem, based on time-frequency images, which are quite modest with data of faulty bearings. The previous solutions have implemented feature selection and extraction based on the parameters of the first component of the processed images.

At this stage, two major improvements could be considered. The first one is based on image analysis and registration. Analysis of the images to be registered shows that it is possible to have images which are very different compared to others from the same class. These must be rejected from the registration process. The second direction, which was promoted in this paper, uses a transformed image that contains contours of the time-frequency image. The selection of the features is based on the statistical moments, as average, variance and squared average values of the areas of the contours. Information based features is also used, by promotion of the Renyi entropy.

The preliminary results show an improvement in the feature space, in the sense of clustering, and the possibility to obtain right classification results based on proposed dissimilarities functions.

In the nearest future a performance comparison of the proposed method with some classical methods based on similarity computation will be considered.

ACKNOWLEDGMENT

The work was partly supported by the Romanian Council for Research (UEFISCDI) under Grant 224/2014, “Experimental model for change detection and diagnosis of vibrational processes using advanced measuring and analysis techniques model-based (VIBROCHANGE)”.

REFERENCES

[1] J. H. Williams, A. Davies, and P. R. Drake (Eds), Condition-based Maintenance and Machine Diagnostics, Springer, 1994.

[2] L. Fedele, Methodologies and Techniques for Advanced Maintenance, Springer, 2011.

[3] M. Bengtsson, E. Olsson, P. Funk, and M. Jackson, "Technical Design of Condition Based Maintenance System", Proceedings of the 8th Congress, University of Tennessee – Maintenance and Reliability Center, Knoxville, USA, May 2nd – 5th, 2004, Paper III.

[4] K. Shin and J. K. Hammond, Fundamental of Signal Processing for Sound and Vibration Eng., John Wiley & Sons Ltd, 2008.

[5] D. M. Yang, A. F. Stronach, and P. MacConnell, "The Application of Advanced Signal Processing Techniques to Induction Motor Bearing Condition Diagnosis", P. Meccanica, Springer, 2003, vol 38(2), pp 297-308.

[6] D. Mironovs and A. Mironov, "Vibration based signal processing algorithm for modal characteristics change assessment", AIP Conference Proceedings 2029, 020043, 2018, pp.1-10.

[7] B. Boashash (Ed), Time-Frequency Signal Analysis and Processing, Elsevier, 2016.

[8] L. Stankovic, M. Dakovic, and T. Thayaparan, Time-Frequency Signal Analysis with Applications, Artech House, 2014.

[9] M. Boufenar, S. Rechak, and M. Rezig, "Time-Frequency Analysis Techniques Review and Their Application on Roller Bearings Prognostics". In: Fakhfakh T., Bartelmus W., Chaari F., Zimroz R., Haddar M. (eds) Condition Monitoring of Machinery in Non-Stationary Operations. Springer, Berlin, Heidelberg, 2012.

[10] D. Aiordachioaie and Th. D. Popescu, "Change Detection by Feature Extraction and Processing from Time-Frequency Images", IEEE 10th Int. Conf. on Electronics, Computers and Artificial Intelligence (ECAI), Iasi, Romania, 2018, pp.1-7.

[11] D. Aiordachioaie, N. Nistor, and M. Andrei, "Change Detection in Time-Frequency Images by Feature Processing in Compressed Spaces", IEEE 24th Int. Symp. for Design and Technology in Electronic Packaging (SIITME), Iași, Romania, 2018, pp.181-186 .

[12] E. Sejdic, I. Djurovic, and J. Jiang, "Time–frequency feature representation using energy concentration: An overview of recent advances", Digital Signal Processing, 19, 2009, pp. 153-183.

[13] Q. Zhu, Y. Wang, and G. Shen, "Comparison and Application of Time-Frequency Analysis Methods for Nonstationary Signal Processing". In: Lin S., Huang X. (eds) Advanced Research on Computer Education, Simulation and Modeling. CESM 2011. Communications in Computer and Information Science, vol 175. Springer, Berlin, Heidelberg, 2011.

[14] M. Karjalainen and V. Pulkki, Communication Acoustics: An Introduction to Speech, Audio and Psychoacoustics, John Wiley & Sons, 2015.

[15] F. Al-Badour, M. Sunar, and L. Cheded, "Vibration analysis of rotating machinery using time–frequency analysis and wavelet techniques", MSSP, vol. 25 (6), 2011, pp. 2083-2101.

[16] M. Akay, Time Frequency and Wavelets in Biomedical Signal Processing, Wiley-IEEE Press, 1997.

[17] P. D. McFadden and W. Wang, Time-Frequency Domain Analysis of Vibration Signals for Machinery Diagnostics. (I) Introduction to the Wigner-Ville Distribution, University of Oxford, Report OUEL 1859/92, 1990.

[18] L. Debnath, The Wigner-Ville Distribution and Time-Frequency Signal Analysis. In: Wavelet Transforms and Their Applications, Birkhäuser, Boston, MA, 2002.

[19] L. Cohen, "Time-Frequency distributions-A review", Proc. IEEE, Vol. 77, pp. 941-981, July 1989.

[20] G. A. Ardeshir, Image Registration Principles, Tools and Methods, Springer, 2012.

[21] I. N. Bankman (Ed.), Handbook of Medical Image Processing and Analysis, Elsevier, 2009.

[22] R. G. Baraniuk, P. Flandrin, A. J. E. M. Janssen, and O. J. J. Michel, "Measuring Time–Frequency Information Content Using the Rényi Entropies", IEEE Transactions on Information Theory, vol. 47(4), 2001, pp. 1391-1409.

[23] Case Western Reserve University, *Bearing Data Center*, At: http://csegroups.case.edu/bearingdatacenter/home, Retrieved: 06, 2019.

[24] D. Aiordachioaie and S. M. Pavel, "Qualitative Analysis of the Time-Frequency Images of Vibrations in Faulty Bearings", IEEE 11th Int. Conf. on Electronics, Computers and Artificial Intelligence (ECAI), Pitesti, Romania, 2019, pp. 1-6.